Liquid Crystals

Publication details, including instructions for authors and subscription information:
http://www.informaworld.com/smpp/title~content=t713926090

Raman studies in SmC$_{FI}$* phases

P. Simeão Carvalho Corresponding author[a]; Yu. I. Yuzyuk[a]; A. Almeida[a]; M. R. Chaves[a]; F. Pinto[a]; C. Da Cruz[b]; H. T. Nguyen[b]

[a] Departamento de Física, IFIMUP, Faculdade de Ciências, Universidade do Porto, 4169-007 Porto, Portugal [b] Centre de Recherche Paul Pascal, Av. A. Schweitzer, 33600 Pessac, France

To cite this Article Carvalho Corresponding author, P. Simeão , Yuzyuk, Yu. I. , Almeida, A. , Chaves, M. R. , Pinto, F. , Da Cruz, C. and Nguyen, H. T.(2004) 'Raman studies in SmC$_{FI}$* phases', Liquid Crystals, 31: 5, 727 — 752

To link to this Article: DOI: 10.1080/02678290410001681573

URL: http://dx.doi.org/10.1080/02678290410001681573

LIQUID CRYSTALS, VOL. 31, NO. 5, MAY 2004, 727–732

Taylor & Francis
Taylor & Francis Group

Raman studies in $\mathrm{SmC}^*_{\mathrm{FI}}$ phases

P. SIMEÃO CARVALHO*, YU. I. YUZYUK†, A. ALMEIDA,
M. R. CHAVES, F. PINTO, C. DA CRUZ‡ and H. T. NGUYEN‡
Departamento de Física, IFIMUP, Faculdade de Ciências, Universidade do
Porto, Rua do Campo Alegre 687, 4169-007 Porto, Portugal.
Tel. 351-22 60 82 645; Fax 351-22 60 82 679
†Faculty of Physics, Rostov State University, Rostov-on-Don, Russia
‡Centre de Recherche Paul Pascal, Av. A. Schweitzer, 33600 Pessac, France

(*Received 8 October 2003; accepted 6 January 2004*)

The study of the Raman intensity of the 'breathing' mode of the benzene rings as a function of the temperature in smectic phases revealed strong anomalies of the intensities I_{ZZ} and I_{YY} in $\mathrm{SmC}^*_{\mathrm{FI2}}$ and $\mathrm{SmC}^*_{\mathrm{FI1}}$ phases, as well as an important shift of the principal optical direction with respect to other smectic phases. The analysis of these results provided evidence for significant structural changes at the SmC*–$\mathrm{SmC}^*_{\mathrm{FI}}$ and $\mathrm{SmC}^*_{\mathrm{FI}}$–$\mathrm{SmC}^*_{\mathrm{A}}$ phase transitions, because the molecules can no longer be treated as cylindrical rods. No anomalies in the tilt angle were found. Experimental results suggest a relationship between the deviation of the optical axis and the particular structure of the $\mathrm{SmC}^*_{\mathrm{FI}}$ phases. The deviation of I_{ZZ} maxima as a function of the rotation angle Ψ and the behaviour evident under an electric field in $\mathrm{SmC}^*_{\mathrm{FI}}$ and $\mathrm{SmC}^*_{\mathrm{A}}$ phases clearly excludes the coexistence of $\mathrm{SmC}^*_{\mathrm{A}}$ and SmC* local domains in $\mathrm{SmC}^*_{\mathrm{FI}}$ phases.

1. Introduction

$\mathrm{SmC}^*_{\mathrm{FI}}$ phases in liquid crystals present an interesting field of research, because of their optical and dielectric properties. As a consequence, they have been studied intensively in recent years [1]. Despite all the experimental results obtained so far, discussion still remains about the molecular arrangement in these phases. To explain the experimental results obtained to date, theoretical models have been proposed [2], based essentially on two conceptual molecular structures: an in-plane distribution of molecules where locally small ferroelectric and antiferroelectric domains coexist (the so-called Ising model) [3]; and an out-of-plane molecular distribution where pairs of neighbouring molecules are strongly coupled (the so-called clock model) [4, 5]. Recently, Mach *et al.* [6] found three-layer and four-layer structures in $\mathrm{SmC}^*_{\mathrm{FI1}}$ and $\mathrm{SmC}^*_{\mathrm{FI2}}$ phases, respectively.

In chiral smectic liquid crystals, Raman spectroscopy has been traditionally used to study the temperature and electric field dependences of the tilt angle [7] and to identify the SmC*–$\mathrm{SmC}^*_{\mathrm{FI}}$ and $\mathrm{SmC}^*_{\mathrm{FI}}$–$\mathrm{SmC}^*_{\mathrm{A}}$ phase transitions [8, 9]. In this work we present a detailed study of Raman spectra obtained in $\mathrm{SmC}^*_{\mathrm{FI}}$ phases of a liquid crystal, that may give a new insight into the structure of these phases.

2. Experimental

The experimental study was performed in a liquid crystal denoted C10FF, which has the chemical formula [10]

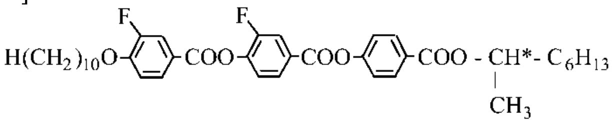

and the phase transition sequence $\mathrm{SmC}^*_{\mathrm{A}}$–$\mathrm{SmC}^*_{\mathrm{FI1}}$–$\mathrm{SmC}^*_{\mathrm{FI2}}$–SmC*–$\mathrm{SmC}^*_{\alpha}$–SmA*–I. The two $\mathrm{SmC}^*_{\mathrm{FI}}$ phases were optically identified but the $\mathrm{SmC}^*_{\mathrm{FI1}}$–$\mathrm{SmC}^*_{\mathrm{FI2}}$ phase transition temperature could not be determined precisely [10].

The liquid crystal was filled by capillary action into a 15.7 μm thick commercial cell from EHC Co., coated with ITO electrodes and rubbed polyimide. A good planar alignment of the liquid crystalline molecules was assured before any measurements, by applying an electric field of about $1\,\mathrm{V\,\mu m^{-1}}$ at 20 Hz for about 30 min in the SmC* phase, close to the SmC*–SmA* phase transition temperature.

Raman spectra were collected by a CCD camera in the backward scattering geometry along the *X*-axis, using a Jobin–Yvon (T64000) spectrometer. The

---

*Author for correspondence; e-mail: psimeao@fc.up.pt

Liquid Crystals ISSN 0267-8292 print/ISSN 1366-5855 online © 2004 Taylor & Francis Ltd
http://www.tandf.co.uk/journals
DOI: 10.1080/02678290410001681573

polarized exciting radiation of a Coherent INNOVA laser (wavelength 5148 Å) was focused on a well-aligned area of the sample. The diameter of the laser spot is estimated ≈3–4 μm. The large numerical aperture (0.55) of the ×50 infinity-corrected microscope objective ensured efficient collection of the scattered light.

The sample was placed inside a specially built oven, where the temperature was controlled by a Lakeshore DRC-93CA temperature controller, with an accuracy better than 0.05 K. The Raman intensity of the 'breathing' mode of the benzene rings, appearing as a doublet at 1602 and 1615 cm^{-1}, was measured as a function of the rotation angle Ψ in the YZ-plane of the laboratory frame of reference, by rotating the sample around the X-axis (figure 1), therefore perpendicular to the glass plates, using a rotational stage attached to the microscope. In the SmA* phase, the maximum Raman intensity is revealed when the local principal direction is oriented with the vector of polarization of the incident and scattered light, which corresponds to $\Psi=0°$.

3. Results and discussion

According to Kim *et al.* [7], if we assume that the average stretching direction of the phenyl rings is parallel to the molecular long axis, the measurements of the Raman intensity of the 'breathing' mode of the benzene rings as a function of the rotation angle Ψ in the YZ plane of the laboratory frame, gives the orientation of the molecules. This fact has been observed experimentally, as the Raman intensity depends on the orientation of the molecular long axis relatively to the polarization plane of the exciting radiation [7–9, 11]. By assuming that our liquid crystal molecules are not really cylindrical rods, but close to it, then as Jen *et al.* [11] point out, we can consider a unique molecular axis, from which we can define a particular molecular reference frame (x,y,z), in which the molecular Raman tensor has the diagonal form [11]

$$\alpha'_{\mathrm{M}}=\alpha_{\mathrm{o}}\begin{pmatrix} a & 0 & 0\\ 0 & b & 0\\ 0 & 0 & 1\end{pmatrix}.$$

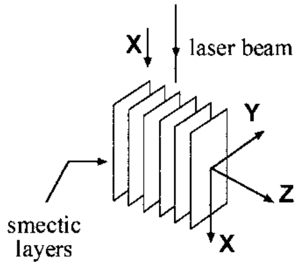

Figure 1. Schematic representation of the smectic layers in the laboratory frame of reference.

Here we shall admit that the z-axis is the direction of the molecular long axis. This Raman tensor is usually strongly anisotropic, so that $a,b \ll 1$ [7, 11].

Using the three Eulerian angles, α (the rotation angle about the average direction of the director, parallel to the smectic layer's normal direction—known as the azimuthal angle), β (the tilt angle of molecules) and γ (the rotation of molecules about the molecular long axis), we can obtain the Raman tensor elements in the laboratory (X, Y, Z) frame, $(\alpha'_{\mathrm{L}})_{ij}$, in terms of the molecular tensor elements $(\alpha'_{\mathrm{M}})_{ij}$.

The exact expressions of $(\alpha'_{\mathrm{L}})_{YY}$ and $(\alpha'_{\mathrm{L}})_{ZZ}$, relating the tensor elements in the laboratory and molecular coordinates, are [11]:

$$\begin{aligned}(\alpha'_{\mathrm{L}})_{YY}=\alpha_0\bigg\{&\frac{1}{2}(a+b)+\left(1-\frac{a+b}{2}\right)\sin^2\beta\sin^2\alpha+\\ &+\frac{1}{2}(a-b)\left[\cos 2\gamma\left(\cos^2\beta\sin^2\alpha-\cos^2\alpha\right)\right.\\ &\left.+\sin 2\gamma\cos\beta\sin 2\alpha\right]\bigg\}\end{aligned}\tag{1}$$

$$\begin{aligned}(\alpha'_{\mathrm{L}})_{ZZ}=\alpha_0\bigg\{&\frac{1}{2}(a+b)+\left(1-\frac{a+b}{2}\right)\cos^2\beta\\ &+\frac{1}{2}(a-b)\sin^2\beta\cos 2\gamma\bigg\}.\end{aligned}\tag{2}$$

As most of the experimental situations are correctly described by assuming that the liquid crystal molecules can be treated as being cylindrical rod-shaped [5] ($a\approx b$), equations (1) and (2) can be considerably simplified, to [9]:

$$(\alpha'_{\mathrm{L}})_{YY}=\alpha_{\mathrm{o}}\left[a+(1-a)\sin^2\alpha\sin^2\beta\right]\tag{3}$$

$$(\alpha'_{\mathrm{L}})_{ZZ}=\alpha_{\mathrm{o}}\left[a+(1-a)\cos^2\beta\right]\tag{4}$$

where the first and the second indices, ij, ($i,j=X$, Y, Z) refer to the directions of the incident and collected polarized light, respectively. As the integrated Raman intensities I_{ij} are proportional to $\langle(\alpha'_{\mathrm{L}})_{ij}{}^2\rangle$, then

$$I_{YY}\propto\left\langle\left[a+(1-a)\sin^2\alpha\sin^2\beta\right]^2\right\rangle\tag{5}$$

$$I_{ZZ}\propto\left\langle\left[a+(1-a)\cos^2\beta\right]^2\right\rangle.\tag{6}$$

3.1. *Raman intensity in the absence of an electric field*

In order to obtain a better understanding of the structure of the different mesophases, we shall compare the experimental intensities I_{ZZ} and I_{YY} with the expressions written in the previous section. To do this analysis it is necessary to know how the spontaneous tilt angle ($\theta=\beta$) behaves as a function

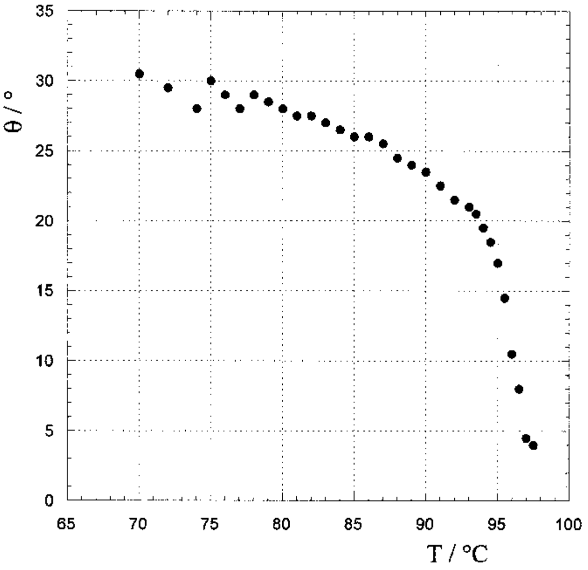

Figure 2. Temperature dependence of the spontaneous tilt angle, taken from reference [10].

of the temperature, in this compound. Figure 2 displays $\theta(T)$, determined by an optical technique, [10]. As can be seen in figure 2, on decreasing the temperature, the tilt angle undergoes a sudden increase at the onset of the SmC* phase, followed by a smooth variation, until it saturates at ~75°C.

The laser beam diameter used here is approximately 3–4 μm, and of the same order of magnitude as the helix pitch in SmC* and $\mathrm{SmC}^*_{\mathrm{A}}$ phases. The helical character of the $\mathrm{SmC}^*_{\mathrm{FI}}$ phases of C10FF, has been shown recently [10] by measuring the rotatory power in these phases, although no value for the pitch was achieved by direct measurements. Furthermore, Shtykov *et al.* [12] obtained for 11OTBBB1M7 helical pitches of 2.8 μm in the $\mathrm{SmC}^*_{\mathrm{FI2}}$ phase, whereas in the $\mathrm{SmC}^*_{\mathrm{FI1}}$ phase the pitch was too high to be measured. Consequently, the measured scattered Raman intensities, in the geometry chosen (see figure 1), are a function of the mean value of $\langle\sin^2\alpha\rangle$, calculated through a length equivalent to the diameter of the laser beam. This means that the measured Raman intensities are expected to be independent of the local values of α, except perhaps in the $\mathrm{SmC}^*_{\mathrm{FI1}}$ phase.

Figure 3 shows the experimental integrated intensities I_{ZZ} and I_{YY} as a function of the temperature, in the different liquid crystalline mesophases. Between 80 and 95°C, i.e. the temperature range of the SmC* phase, the experimental results are correctly described by expressions (5) and (6), i.e. can be fitted to the data, by taking the $\theta(T)$ values shown in figure 2 and by assuming $\langle\sin^2\alpha\rangle$ to be independent of the temperature. In terms of symmetry, we can state that macroscopically the structure 'seen' by Raman scattering has a $C_{\infty v}$ group, and then the phase has 'uniaxial' behaviour.

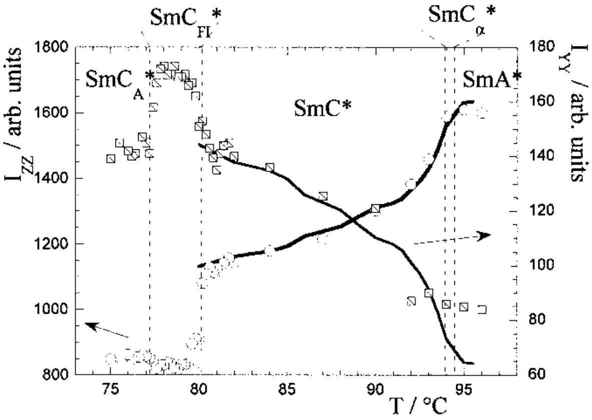

Figure 3. Integrated Raman intensities I_{ZZ} and I_{YY} as functions of temperature. The dotted lines indicate the phase transitions. The full lines in the SmC* phase are fits of equations (5) and (6) to experimental data, taking into account the tilt angle measurements shown in figure 2. The fitting parameters obtained are: $a(=b)=0.199$; $\langle\sin^2\alpha\rangle=0.574$.

On lowering the temperature, the onset of the $\mathrm{SmC}^*_{\mathrm{FI}}$ phases is very clearly marked by a sudden decrease of I_{ZZ} and a steep increase of I_{YY}. In this temperature range no anomalies are found in $\theta(T)$ (figure 2), and consequently the sudden decrease of I_{ZZ} cannot be attributed to a visible change of the tilt angle. A decrease of intensity could also originate from thermal fluctuations, leading to some type of disorder in the system. However this explanation has to be discarded: if this situation had happened we would also observe a decrease in the intensity of I_{YY}, which effectively does not occur. The most plausible explanation for the observed behaviour is to assume a drastic change of the liquid crystalline structure at 80°C, with a significant change of the macroscopic symmetry, which is detected by the Raman technique.

Some of the properties of SmC* phase are described by expressions (3) and (4), which were deduced from expressions (1) and (2), respectively, by assuming that the molecules can be treated as cylindrical rods. This last hypothesis seems not to be valid in the $\mathrm{SmC}^*_{\mathrm{FI}}$ phases, and therefore the changes in I_{ZZ} are very probably related to the loss of rotational symmetry in the average positions of the molecules, resulting in a further change of the mean value of $\cos 2\gamma$. In particular, a change of the optical axis at the SmC*–$\mathrm{SmC}^*_{\mathrm{FI2}}$ phase transition is expected. The data shown in figure 4 corroborate this expectation. I_{ZZ} is presented as a function of the rotation angle (Ψ), for different temperatures, the maximum of each curve occurring for the local principal direction. In the $\mathrm{SmC}^*_{\mathrm{A}}$ and SmC*

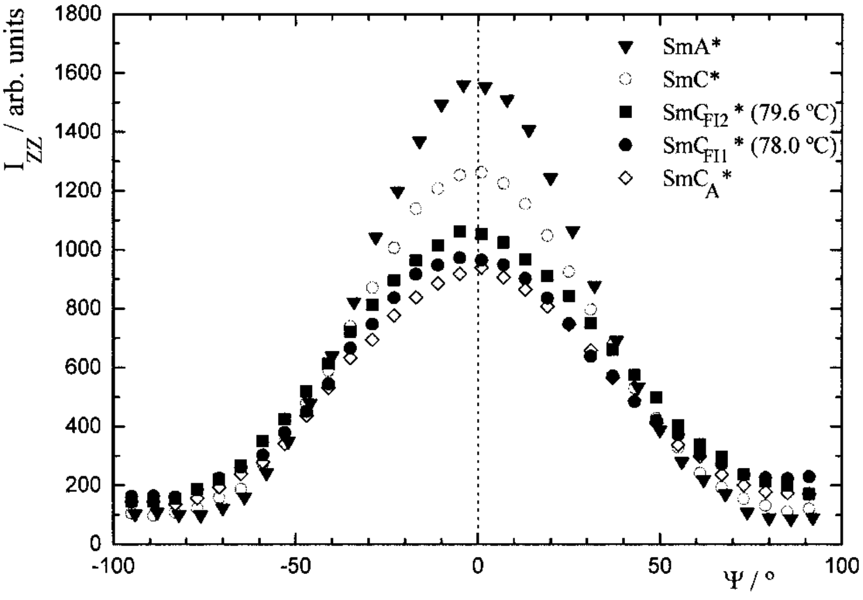

Figure 4. Integrated Raman intensity I_{ZZ} as a function of the rotation angle Ψ, in several smectic phases in the absence of electric field; Ψ was measured in the YZ-plane.

phases, the maximum of I_{ZZ} is obtained for $\Psi=0$, i.e. this maximum occurs at the direction of the I_{ZZ} maximum of the non-tilted SmA* phase. For the SmC$^*_{\mathrm{FI}}$ phases the I_{ZZ} maximum is systematically shifted up to $\Psi \sim 6°$.

3.2. *Influence of an electric field*

One of the most important features of Raman measurements is the sensitivity to orientational changes in the direction of the molecular core in liquid crystals. As different liquid crystalline phases respond differently to an electric field, we have measured the I_{ZZ} Raman intensity in all phases as a function of the rotation angle Ψ, for several electric fields. The results are shown in figure 5, obtained with a cell of 15.7 µm thickness. In the SmC* phase, figure 5 (*a*), an electrical voltage as low as 10 V is enough to induce the tilt saturation. No threshold field was found in this phase.

We shall now focus attention on the SmC$^*_{\mathrm{FI}}$ phases. As far as could be seen, no significant threshold field was detected in the SmC$^*_{\mathrm{FI1}}$ and SmC$^*_{\mathrm{FI2}}$ phases. In both phases, the maximum rotation of the principal optical direction is $\approx 27°$, obtained for about 20 V, figures 5 (*b*) and 5 (*c*), and is consistent with the spontaneous tilt angle in these phases (figure 3); the increase of I_{ZZ} intensity in the SmC$^*_{\mathrm{FI1}}$ phase, figure 5 (*c*), between 20 and 30 V, suggests an improvement of molecular alignment, as the angle Ψ for maximum I_{ZZ} remains unchanged for fields above 20 V.

In the SmC$^*_{\mathrm{A}}$ phase, a threshold voltage of about 20 V appears and tilt saturation can only be achieved for 40 V and higher (Figure 5 (*d*)).

4. Conclusion

The existence of important anomalies in the Raman intensities I_{ZZ} and I_{YY}, at the SmC*–SmC$^*_{\mathrm{FI2}}$ and SmC$^*_{\mathrm{FI1}}$–SmC$^*_{\mathrm{FI2}}$ phase transitions, is clearly associated with a local molecular rearrangement. For a large number of experimental situations, liquid crystal molecules behave as cylindrical rods, which means that on average there is rotational symmetry about their long axis. This symmetry is closely related to the structure of the liquid crystalline phase but suffers a significant change in SmC$^*_{\mathrm{FI}}$ phases. As a result, a deviation of the principal optical direction in SmC$^*_{\mathrm{FI1}}$ and SmC$^*_{\mathrm{FI2}}$ phases relative to that shown in SmA*, SmC* and SmC$^*_{\mathrm{A}}$ phases is observed. Raman measurements of I_{ZZ} as a function of the rotation angle clearly reveal such a local deviation in SmC$^*_{\mathrm{FI1}}$ and SmC$^*_{\mathrm{FI2}}$ phases. Consequently, the behaviour shown by $I_{ZZ}(\Psi)$ in SmC$^*_{\mathrm{FI}}$ phases disproves the hypothesis of coexistence of SmC* and SmC$^*_{\mathrm{A}}$ local domains.

The interpretation of the results obtained in Raman scattering suggests that the observation of conoscopic figures should reveal the biaxial character of SmC$^*_{\mathrm{FI}}$ phases. The small deviation of the principal optical axes ($\sim 6°$) can explain the difficulty in observing this effect.

It is well known that the orientation of molecules in liquid crystals under the influence of a d.c. electric field is different in SmC*, SmC$^*_{\mathrm{FI}}$ and SmC$^*_{\mathrm{A}}$ phases. To understand the behaviour in SmC* and SmC$^*_{\mathrm{A}}$ phases

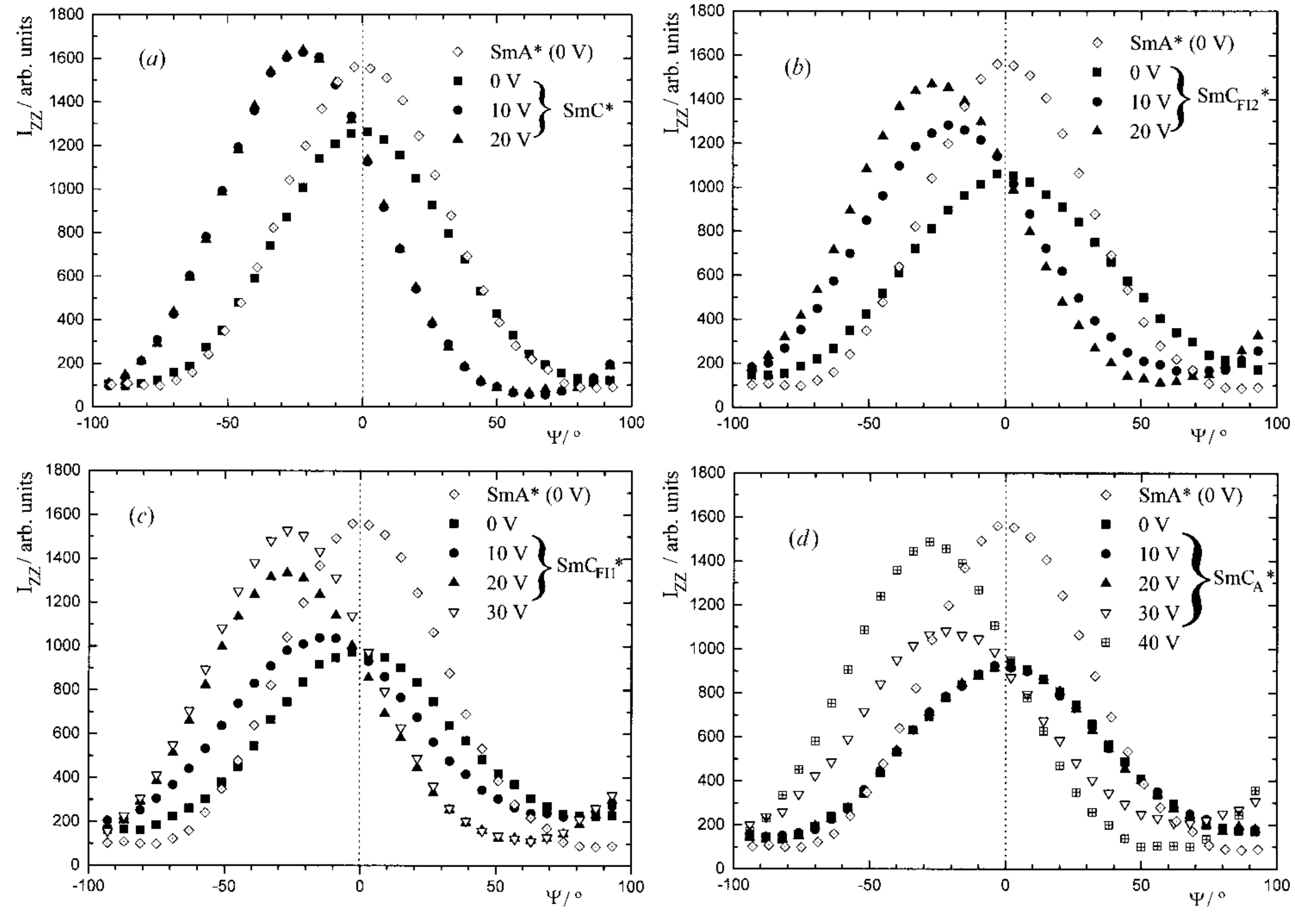

Figure 5. Integrated Raman intensity I_{ZZ} as a function of the rotation angle Ψ, for several applied electric fields. The results were obtained in (*a*) SmC*, (*b*) SmC^*_{FI2}, (*c*) SmC^*_{FI1} and (*d*) SmC^*_A phases, and compared with the curve obtained in the SmA* phase in the absence of an electric field.

under an electric field, we must take into account the coupling between the in-plane polarization arising near the smectic layer boundaries, and the electric field. According to [13], this in-plane polarization is nearly parallel to the molecular tilt plane in the SmC^*_A phase (see also [14]) and perpendicular to it in the SmC* phase. Consequently, a low electric field can unwind the helicoidal structure of an SmC^*_A phase, so that the tilt plane becomes parallel to the field [11]; but in order to induce the ferroelectric arrangement, the liquid crystal frame of reference has to rotate 90°, which can only be accomplished for a sufficiently high threshold electric field.

In SmC^*_{FI} phases, such a threshold field was not evident in our experiments. Moreover, the increase of the saturation field from SmC^*_{FI2} to SmC^*_{FI1} phase, can be attributed to the change from a four-layer to a three-layer structure in these phases, respectively, the latter being more difficult to unwind completely. Near the SmC^*_A –SmC^*_{FI1} phase transition, the lowest voltage required to induce a ferroelectric orientation in the SmC^*_{FI1} phase ($\approx$20 V) is almost the threshold voltage measured in the SmC^*_A phase.

These Raman studies confirm the existence of a high threshold electric field only in the SmC^*_A phase; they also show that the saturation field in the SmC^*_{FI1} and SmC^*_{FI2} phases is much smaller than in the SmC^*_A phase; namely, the lowest voltage to induce a ferroelectric orientation in the SmC^*_{FI1} phase ($\approx$20 V) is almost the threshold voltage measured in the SmC^*_A phase. Therefore, these results clearly exclude the possible coexistence of local SmC^*_A and SmC* domains in SmC^*_{FI} phases and provide evidence for significantly different structural properties for SmC^*_{FI} phases relative to SmC^*_A and SmC* phases.

This work was supported by the project PRAXIS XXI /3/3.1/MMA/1769/95. Yu. I. Y. and F. P. thank project PRAXIS XXI for their grants (respectively BCC/4463/96 and BIC J/4688/96).

References

[1] Fukuda, A., Takanishi, Y., Isozaki, T., Ishikawa, K., and Takezoe, H., 1994, *J. mater. Chem.*, **4,** 997.

[2] Sun, H., Orihara, H., and Ishibashi, Y., 1993, *J. phys. Soc. Jpn.*, **62,** 2706.

[3] Takezoe, H., Lee, J., Ouchi, Y., and Fukuda, A., 1991, *Mol. Cryst. liq. Cryst.*, **202,** 85.

[4] Škarabot, M., Čepič, M., Zekš, B., Blinc, R., Heppke, G., Kityk, A. V., and Muševič, I., 1998, *Phys. Rev. E*, **58,** 575.

[5] Lorman, V. L., 1995, *Mol. Cryst. liq. Cryst.*, **262,** 437; Lorman V. L., 1996, *Liq. Cryst.*, **20,** 267.

[6] Mach, P., Pindak, R., Levelut, A.-M., Barois, P., Nguyen, H. T., Huang, C. C., and Furenlid, L., 1998, *Phys. Rev. Lett.*, **81,** 1015.

[7] Kim, K. H., Miyachi, K., Ishikawa, K., Takezoe, H., and Fukuda, A., 1994, *Jpn. J. appl. Phys.*, **33,** 5850.

[8] Farhi, R., Sidir, M., and Nguyen, H. T., 1995, *J. Phys. Fr.*, **5,** 1793.

[9] Yuzyuk, Yu. I., Sarmento, S., Simeão Carvalho, P., Almeida, A., Pinto, F., Chaves, M. R., and Nguyen, H. T., 1999, *Liq. Cryst.*, **26,** 1805.

[10] Da Cruz, C., Rouillon, J. C., Marcerou, J. P., Isaert, N., and Nguyen, H. T., 2001, *Liq. Cryst.*, **28,** 125.

[11] Jen, S., Clark, N. A., and Pershan, P. S., 1977, *J. chem. Phys.*, **66,** 4635.

[12] Shtykov, N. M., Vij, J. K., and Nguyen, H. T., 2001, *Phys. Rev. E*, **63,** 051708.

[13] Matsumoto, T., Fukuda, A., Johno, M., Motoyama, Y., Yui, T., Seomun, S. S., and Yamashita, M., 1999, *J. mater. Chem.*, **9,** 2051.

[14] Miyachi, K., Matsushima, J., Takanishi, Y., Ishikawa, K., Takezoe, H., and Fukuda, A., 1995, *Phys. Rev. E*, **52,** R2153.